

# FTIR Measurements of Stratospheric Gases at the St. Petersburg Site



Yana Virolainen , Alexander Polyakov , Yury Timofeyev ,  
and Anatoly Poberovsky 

**Abstract** Ozone anomalies that occur during winter-spring periods in the Northern Hemisphere have been increasingly observed in recent decades not only in polar, but also in mid-polar regions, including territories of megacities. Regular monitoring of stratospheric gases involved in ozone-depleting processes is essential for predicting the appearance of ozone mini-holes and the growth of UV surface illumination. Long-term ground-based FTIR (Fourier Transform Infrared) measurements have been performed at the St. Petersburg site (60N, 30E) since 2009. The location of St. Petersburg near the border of mid and high latitudes allows to observe the stratospheric gases variations under different atmospheric conditions, including polar vortex intrusion. We analyzed time series of O<sub>3</sub>, HNO<sub>3</sub>, ClONO<sub>2</sub>, HCl, and HF atmospheric measurements at the St. Petersburg site in 2009–2022, compared them with independent satellite measurements (ACE-FTS) and demonstrated the capabilities of ground-based FTIR method to study and explain the temporal variability of the stratospheric trace-gases in winter-spring period of 2016.

**Keywords** FTIR · Stratospheric gases · Atmospheric remote sensing

## 1 Introduction

After discovery of the Antarctic ozone hole in the 1980s the investigation of ozone depletion has been enhanced [1]. In recent decades, the study of ozone loss in the Arctic came also into the focus of research since the ozone anomalies in winter-spring periods in the Northern Hemisphere have been increasingly observed not only in the polar, but also in the mid-polar regions [2–4]. In addition to ozone observation, it is very important to monitor the changes in the abundancies of stratospheric gases involved in ozone depletion cycle to predict the development of the ozone layer and the increase of UV radiation at the surface [5].

---

Y. Virolainen (✉) · A. Polyakov · Y. Timofeyev · A. Poberovsky  
St. Petersburg University, Universitetskaya Emb., 7-9, 199034 St. Petersburg, Russia  
e-mail: [yana.virolainen@spbu.ru](mailto:yana.virolainen@spbu.ru)

Ground-based FTIR (Fourier transform infrared) measurements of solar radiation transmitted through the atmosphere can be used to investigate the variability of stratospheric gases with high temporal resolution. In the framework of the NDACC (Network for the Detection of Atmospheric Composition Change), dozens of observational sites around the globe are equipped with FTIR spectrometers of high spectral resolution [6]. Bruker IFS 125 HR spectrometer at the St. Petersburg site located at Peterhof campus of St. Petersburg University is the only instrument of such type in Russia that is certified by the Infra-Red Working Group (IRWG) of the NDACC network. The location of the St. Petersburg site ( $59^{\circ}53'$  N,  $29^{\circ}50'$  E, 20 m a.s.l.) near the border of mid and high latitudes allows stratospheric gases variations to be observed at different temporal scales and under various atmospheric conditions, including polar vortex intrusion. Ozone and ozone-related species  $\text{HNO}_3$ ,  $\text{ClONO}_2$ ,  $\text{HCl}$ , and  $\text{HF}$  are the trace gases required by IRWG to be measured at the NDACC IRWG sites [7]. In the current study, we present and analyze the variability of stratospheric gases measured by FTIR method at the St. Petersburg site.

## 2 Measurements of Trace Gases

### 2.1 FTIR Data

FTIR measurements using Bruker IFS 125 HR spectrometer are performed at the St. Petersburg site since the beginning of 2009. Weather in St. Petersburg is highly variable with frequent air-mass changes: approximately 165 overcast days and 140 days of cyclonic activity per year. FTIR method uses the Sun as a light source, thus spectra are recorded under cloudless conditions or in the cloud breaks only, which gives 60–70 days of measurements per year, mainly in spring and summer seasons.

We analyze the spectra measured with  $0.005\text{ cm}^{-1}$  spectral resolution in  $650\text{--}5400\text{ cm}^{-1}$  spectral range (covered by 3 different optical filters) with PROFFIT96 ( $\text{O}_3$ ,  $\text{HNO}_3$ ,  $\text{ClONO}_2$ ) and SFIT4 ( $\text{HCl}$ ,  $\text{HF}$ ) software routinely used at the NDACC IRWG sites [8]. The details of the retrieval strategies applied can be found in [9–11]. We retrieve target gases profiles first, then integrate them to derive total columns (TCs). Time series of TC measurements of stratospheric gases have been already used in validation of various satellite data [9, 10, 12, 13, 15] and in comparisons with the results of numerical modelling [10, 11, 14, 15].

Table 1 summarizes the statistical characteristics of FTIR-measurements at the St. Petersburg site in the period of 2009–2022. The differences in number of days and measurements for target gases are explained by:

- different number of measurements performed in  $650\text{--}1400\text{ cm}^{-1}$  ( $\text{O}_3$ ,  $\text{HNO}_3$ ,  $\text{ClONO}_2$ ),  $1700\text{--}3400\text{ cm}^{-1}$  ( $\text{HCl}$ ), and  $2350\text{--}5400\text{ cm}^{-1}$  ( $\text{HF}$ ) spectral ranges;
- different criteria for selection high-quality spectra and measurements [9–12].

**Table 1** Statistics of stratospheric gases TCs retrieval at the St.Petersburg site in 2009–2022 (st—statistical, sys—systematic, meas—measurements)

Target gas	N days (N meas)	DOFS	Error st, %	Error sys, %	Trend, % yr <sup>-1</sup>
O <sub>3</sub>	789 (5220)	4.3 ± 0.3	2.2 ± 0.6	3.0 ± 0.5	+ 0.02 ± 0.20
HNO <sub>3</sub>	779 (5182)	3.1 ± 0.4	4.0 ± 2.1	9.3 ± 1.7	+ 0.23 ± 0.34
ClONO <sub>2</sub>	751 (4158)	1.02 ± 0.07	22 ± 9	28 ± 8	-1.64 ± 0.85
HCl	907 (5788)	2.5 ± 0.2	2.3 ± 0.7	5.4 ± 0.2	-0.22 ± 0.21
HF	950 (6403)	2.6 ± 0.3	2.2 ± 2.3	5.7 ± 5.4	+ 0.47 ± 0.25

The number of DOFS (degrees of freedom for signal) describes the information content of spectroscopic measurements with respect to a target gas. It is calculated as a trace of the averaging kernel matrix [16]. Therefore, it is possible to retrieve 3–4 independent pieces of information on vertical structure for O<sub>3</sub> and HNO<sub>3</sub>, 1–2 pieces for HF and HCl, and only one piece for ClONO<sub>2</sub> (its total column).

The error estimation is based on the formalism suggested by Rodgers [16] and is included in the retrieval codes [8]. There we consider two types of errors: (a) errors due to uncertainty of the input parameters (instrumental characteristics, spectroscopic data, temperature profile, etc.), and (b) errors due to the measurement noise. Spectroscopic data uncertainty refers to systematic errors only, as it is constant between consecutive measurements. Measurement noise is a statistical error, uncorrelated in time. Other uncertainties considered may contribute to both statistical and systematic errors.

Due to weak absorption lines in measured solar spectra, errors for ClONO<sub>2</sub> TC retrieval are the largest (20–30%); both systematic and statistical errors are mainly determined by uncertainty in the baseline of a spectrum which includes continuum absorption of interfering gases, aerosol extinction, quasi-harmonic distortion in spectra, etc. [17]. The changes in a signal recorded due to the absorption of ClONO<sub>2</sub> do not exceed 1–2% in the period of its maximal abundancies in the atmosphere (in winter-spring season). At the same time, the standard level of measurement noise account for 0.7–1% of a signal. Therefore, in the rest of a year, ClONO<sub>2</sub> measurement errors as a rule are greater than 100%. Statistical and systematic measurement errors for other target gases do not exceed 2–9%. See for details the error budget of FTIR retrievals at the St. Petersburg site in [18].

## 2.2 Analysis of Time Series

To analyze the variability in TCs of target gases on a scale of both long-term trends and seasonal variability, we used the approach based on the approximation of a series of data by expansion on a finite-dimensional basis. This approach is described in detail in [19]. Last column of Table 1 presents trend values for

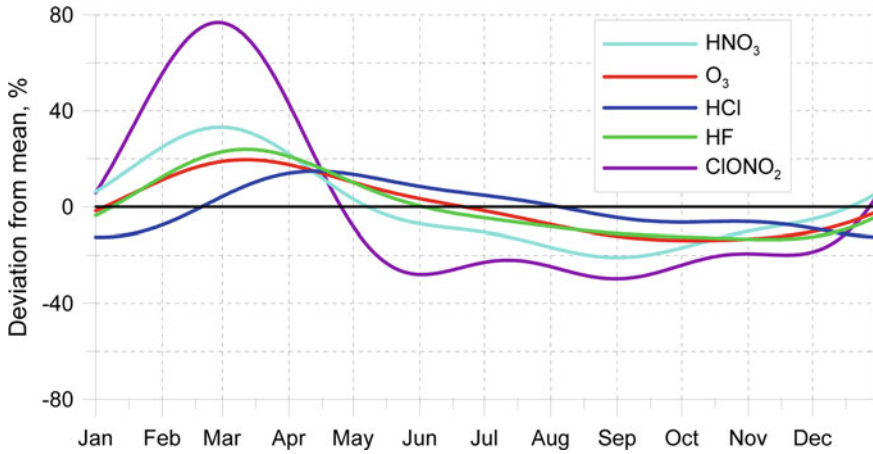


**Fig. 1** Seasonal cycle of the variability in stratospheric gases TCs at the St. Petersburg site

TCs time series estimated by subtracting the seasonal variability from initial time series. Within the 95% confidence interval, statistically significant negative trend is observed for  $\text{ClONO}_2$  ( $-1.64\% \text{ yr}^{-1}$ ) and  $\text{HCl}$  ( $-0.22\% \text{ yr}^{-1}$ ), and positive trend for  $\text{HF}$  ( $+0.47\% \text{ yr}^{-1}$ ).

To describe a seasonal cycle, we modeled the intra-annual variability in terms of a Fourier series considering periodicities of 4 months and larger [19]. Figure 1 depicts seasonal relative variability in TCs of target gases for the St. Petersburg site. The largest variability, which reach in maximum  $\sim 80\%$  at the end of winter and the beginning of spring, is observed for  $\text{ClONO}_2$ .  $\text{HNO}_3$  maximum of  $\sim 30\%$  relates to the same period, whereas  $\text{O}_3$  and  $\text{HF}$  maxima of  $\sim 20\%$  are shifted to the mid of March. The smallest variability is observed in  $\text{HCl}$  TCs; it does not exceed 15–18% for the mid of spring.

### 2.3 Comparison with ACE-FTS Measurements

The ACE-FTS is a high spectral resolution ( $0.02 \text{ cm}^{-1}$ ) Fourier transform spectrometer operating in  $750\text{--}4400 \text{ cm}^{-1}$  spectral range. The instrument is a main payload on board the SCISAT-1 satellite, with a drifting orbit, an inclination of  $73.9^\circ$ , and an altitude of 650 km. Working primarily in a solar occultation mode, the satellite provides information on vertical profiles (typically 10–100 km) for temperature, pressure, and for dozens of atmospheric gases over the latitudes of  $85^\circ \text{ N}$  to  $85^\circ \text{ S}$ . The lower boundary of the retrieved profiles is above 7–8 km, and the errors at the lower level may be greater than in the rest of the profile.

For comparison with FTIR-measurements, we used operational version v.4.1/4.2 of ACE-FTS data; the retrieval algorithm is described in [20]. We selected the ACE-FTS measurements closer than 500 km from the St. Petersburg site and integrated profiles from 14.5 to 41.5 km. Due to the peculiarity of the orbit and the weather conditions at the St. Petersburg site, SCISAT-1 measurements are available on rare occasions, mainly in winter and spring. We took daily averaged FTIR data and compared them with the available ACE-FTS measurement at the same day. As the number of DOFS for O<sub>3</sub> and HNO<sub>3</sub> is greater than 3, we first integrated the profiles retrieved in 3 atmospheric layers and then compared FTIR columns in 15–50 km layer with ACE-FTS data. The layers were selected in accordance with the DOFS values (greater than unit for each layer). For other target gases, we considered the FTIR TC retrievals. The number of data pairs for each target gas is presented in Table 2.

We observe the highest correlations (0.87–0.90) for O<sub>3</sub> and HNO<sub>3</sub> stratospheric columns that can be partly explained by nearly the same atmospheric layer taken for consideration. Standard deviation of differences (SDD) for all target gases do not exceed the total measurement errors of both instruments. It means that both methods describe the temporal variability in target gases in the same way. The large positive bias in HCl and HF data is due to differences in total columns (FTIR) and stratospheric columns (ACE-FTS) of these gases. The negative bias in ClONO<sub>2</sub> data and large SDD may be caused by low sensitivity of FTIR data to changes in stratospheric abundancies of ClONO<sub>2</sub> and consequently the large measurement errors except period of winter-spring maximum (see Fig. 1). In current comparisons, we do not study separately cases when FTIR and ACE-FTS instruments observe different airmasses. In winter periods, it can significantly influence on the results of comparison as one airmass may be inside of polar vortex whereas another—outside.

**Table 2** FTIR vs. ACE-FTS comparison at the St. Petersburg site. FTIR data are taken as a reference for calculation of relative differences ( $\Delta$ —bias, SDD—standard deviation of differences,  $R_{\text{corr}}$ —correlation coefficient)

Target gas	N of data pairs	$\Delta \pm \text{SDD}$		$R_{\text{corr}}$
O <sub>3</sub>	93	$5 \pm 14 \text{ DU}$	$2.0 \pm 5.0\%$	$0.90 \pm 0.02$
HNO <sub>3</sub>	79	$(0.7 \pm 1.3) \times 10^{+15} \text{ cm}^{-2}$	$4.6 \pm 8.8\%$	$0.87 \pm 0.03$
ClONO <sub>2</sub>	69	$(-0.8 \pm 3.1) \times 10^{+14} \text{ cm}^{-2}$	$-8 \pm 33\%$	$0.62 \pm 0.08$
HCl	100	$(1.1 \pm 0.4) \times 10^{+15} \text{ cm}^{-2}$	$26 \pm 9\%$	$0.65 \pm 0.06$
HF	102	$(1.9 \pm 2.6) \times 10^{+14} \text{ cm}^{-2}$	$10 \pm 14\%$	$0.58 \pm 0.07$

### 3 Analysis of Ozonosphere

#### 3.1 Role of Chlorines in Ozone Destruction

The variability in the ozone layer in polar stratosphere is substantially controlled by the presence and variations in the content of chlorine radicals in the atmosphere [21]. The composition of the stratosphere is usually determined by chemical reactions in the gas phase, and chlorine is mainly found in the form of HCl and ClONO<sub>2</sub>. At low temperatures (below 195 K), in heterogeneous reactions on the surface of polar stratospheric clouds (PSC) particles the reservoir chlorine compounds HOCl and Cl<sub>2</sub> are released. In the presence of solar radiation, they form active chlorine Cl, which destroys ozone molecules in the catalytic cycle [22]. After the stratospheric temperature increases and the PSC and sulfate aerosol particles disappear, the ClONO<sub>2</sub> and HCl reservoir-gas content is restored. The rate of chlorine deactivation in ClONO<sub>2</sub> depends on the NO<sub>2</sub>, which is formed during the photolysis of HNO<sub>3</sub> in the gas phase. In the absence of HNO<sub>3</sub> in the gas phase, active chlorine does not pass into inert ClONO<sub>2</sub>, which leads to an even greater increase in the chemical destruction of ozone. The distribution of inactive chlorine among the reservoir gases plays an important role, since ClONO<sub>2</sub> molecules during photolysis can lead to the secondary formation of active chlorine. The movement of air masses with a high ClONO<sub>2</sub> content outside the polar vortex can cause ozone destruction in midlatitudes in late spring [23].

The described mechanism of the chemical destruction of ozone is typical for polar latitudes in the presence of polar vortex, prolonged low temperatures of the lower stratosphere, and the presence of PSC. However, with the penetration of polar vortex into midlatitudes and its subsequent destruction, this mechanism may also indirectly affect a decrease in the stratospheric ozone content in midlatitudes.

#### 3.2 Study of Ozonosphere over St. Petersburg with FTIR-method

Opposite to the Antarctic, in the Arctic and adjacent regions evolution of the ozone layer in winter-spring seasons is usually dominated by dynamic processes [22]. To study the ozone layer and to quantify ozone losses, it is necessary to distinguish effects due to chemical processes from dynamic transport and mixing of air masses. Due to inactivity and long lifetime HF molecules are not directly involved in chemical reactions. Therefore, HF TCs are often used as a tracer of dynamic processes in the stratosphere [24]. The vertical profiles of ozone and ozone-related stratospheric gases usually correlate well with the HF profile in the lower stratosphere with maximal abundancies of these gases, thus vertical movements in the stratosphere will proportionally change TCs for both HF and other stratospheric gases considered.

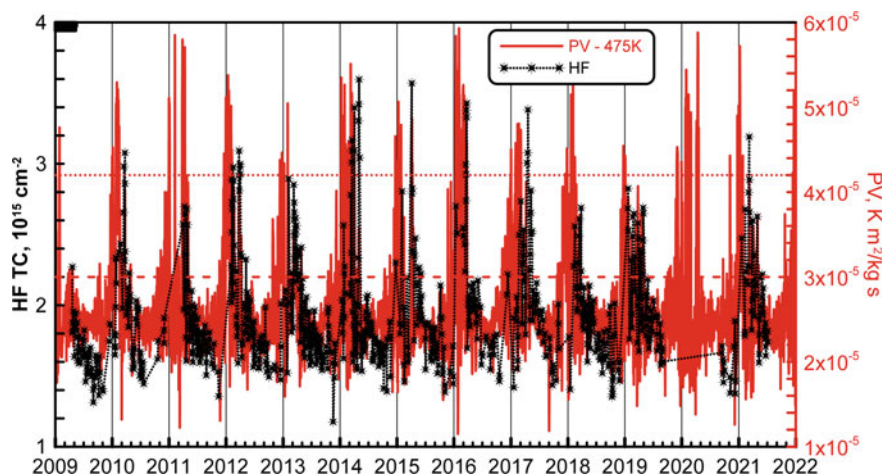


**Fig. 2** Time series of HF TCs measured at the St. Petersburg site and the PV values at the potential temperature level of 475 K. The dashed line on the PV scale indicates the edge of polar vortex, the dotted line indicates airmasses inside polar vortex

Figure 2 presents the time series of the HF TCs derived at the St. Petersburg site between 2009 and 2022, along with the values of the potential vorticity (PV) at the isentropic level of the potential temperature of 475 K, which is one of the indicators of the polar vortex intensity. The PV data are taken from the ERA5 reanalysis data [25], daytime climatology, referred to 12:00 GMT for the St. Petersburg site. The 475 K potential temperature level correspond to the 18–20 km altitudes where the largest local ozone losses are typically found in the Arctic springs [22]. As a rule, the air mass is considered to be inside polar vortex if PV exceeds  $4.2 \text{ K m}^2/\text{kg s}$  [26].

HF TCs correlate well with the PV values. For 1002 days of HF TC measurements at the St. Petersburg site, the correlation coefficient between the PV and HF TCs totals  $0.55 \pm 0.03$ . The PV has the maximal values mainly in January. In the presence of observations, the winter maxima of HF TCs coincide in time with the PV maxima. In most years, spring maxima of HF TCs are also observed, not always consistent with the PV maxima. PV values considered are determined only at one level in the atmosphere, whereas HF TCs refer to the whole atmosphere. Therefore, the use of the HF TCs as a dynamic factor is more relevant than use of PVs to define the dynamics of the ozonosphere. The maximal values of HF TCs characterize the air masses located inside polar vortex. In [27], for another subpolar station of the NDACC network Kiruna ( $67.8^\circ \text{ N}$ ) it was shown that, despite significant correlations between the HF TCs and the PV values, even with low PV values (less than  $3 \text{ K m}^2/\text{kg s}$ ), the air mass can be inside polar vortex, which is more accurately determined by the HF TC value when it exceeds  $2.5 \cdot 10^{15} \text{ cm}^{-2}$ .

Analyzing Fig. 2, we can say that atmosphere over St. Petersburg in some years is characterized by two periods of possible intrusion of polar vortex—in the middle of

winter (January) and in the beginning of spring (March–April). As FTIR measurements at the St. Petersburg site are carried out only in the presence of direct solar radiation, and winters are characterized by the predominance of cyclonic activity; it is not possible to study the ozone layer evolution by FTIR-method every year [28].

In the winter of 2015/2016, an unusually sharp and repeated decrease in ozone TCs and record low values of the temperature of the stratosphere were observed in the Arctic and adjacent regions [29]. Temperature minima were observed from December 2015 to early February 2016, when the temperature dropped below the threshold for the formation of PSCs for a long time, which led to the removal of  $\text{HNO}_3$  molecules from the gas phase and their deposition on PSC particles, that is, to the denitrification of the stratosphere [29]. The extremely cold and strong polar vortex affected not only polar, but also the subpolar (middle) latitudes. Major sudden stratospheric warming in March ended the Arctic winter.

Figure 3 demonstrates the time dependence of the variability in ratio of ozone and ozone-related gases to HF TCs at the St. Petersburg site in winter-spring period of 2016. Weather conditions allowed the FTIR measurements to be performed at the St. Petersburg site only for 2 days in January: 14 and 22, and 6 days in March 2016. In addition to stratospheric gases measurements, Fig. 3 highlights the periods of possible intrusion of polar vortex in the atmosphere over St. Petersburg (horizontal lines in columns) and the periods when the stratospheric temperature dropped below the threshold values for the formation of PSC (vertical lines in columns). The detailed analysis of the evolution of ozonosphere at the St. Petersburg site was discussed in [28]. There we will only summarize that the winter of 2016 is characterized by a cold stratosphere and a stable polar vortex observed over St. Petersburg, accompanied by the chlorine activation and denitrification of the stratosphere, leading in some periods to chemical ozone losses in March 2016 detected by FTIR method at the St. Petersburg site.

## 4 Conclusions

We have presented the ground-based FTIR-method which uses measurements of solar radiation by Bruker IFS 125 HR spectrometer at the St. Petersburg site. We have analyzed time series of ozone and ozone-related gases ( $\text{HNO}_3$ ,  $\text{ClONO}_2$ ,  $\text{HCl}$ , and  $\text{HF}$ ) measured in 2009–2022.

We detected the maxima of seasonal cycle of variability in all gases considered in spring periods, varying from 15% for  $\text{HCl}$  to  $\sim 80\%$  for  $\text{ClONO}_2$ . For the period considered, statistically significant trends were observed only in  $\text{ClONO}_2$  ( $-1.64\% \text{ yr}^{-1}$ ),  $\text{HCl}$  ( $-0.22\% \text{ yr}^{-1}$ ), and  $\text{HF}$  ( $+0.47\% \text{ yr}^{-1}$ ) TCs.

The comparison of FTIR data with satellite ACE-FTS measurements in 14.5–41.5 km layer demonstrates their good correlations varying from 0.87–0.90 for  $\text{O}_3$  and  $\text{HNO}_3$  stratospheric columns to 0.58–0.65 for  $\text{HCl}$ ,  $\text{HF}$ , and  $\text{ClONO}_2$  TCs. Standard deviation of differences for all gases do not exceed the total measurement errors of both instruments.



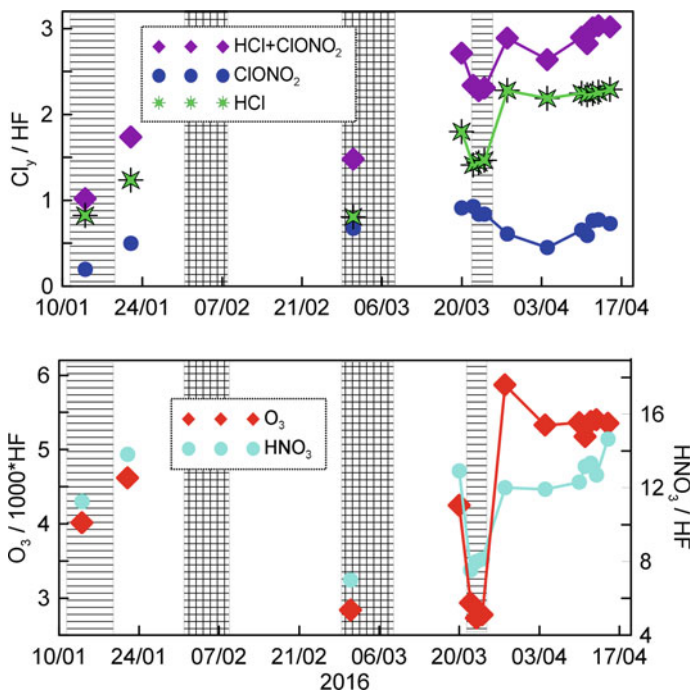


**Fig. 3** Time series of the ratio of HCl, ClONO<sub>2</sub>, and their sum to HF TCs (top) and the ratio of HNO<sub>3</sub> to HF TC and O<sub>3</sub> TC to 1000\*HF TC (bottom) in 2016 according to FTIR measurements at the St. Petersburg site. The columns with horizontal lines highlight the period of the potentially possible penetration of the polar vortex into the stratosphere over St. Petersburg. The vertical lines in the columns indicate the periods of possible occurrence of the PSC

We have demonstrated the capabilities of the ground-based FTIR method to study the short-term temporal variability of the stratospheric gases involved in the cycles of destruction and formation of the ozone layer, to detect the periods of chemical ozone loss, and, therefore, to study the ozone layer evolution.

The time series of ground-based FTIR measurements of stratospheric gases can be used for validation of satellite measurements as well as for improvement of the regional atmospheric chemistry-climate models.

**Acknowledgements** FTIR-measurements were carried out on the equipment of the Geomodel resource center of St. Petersburg State University. The study of the variability of stratospheric gases at the St. Petersburg site was supported by the Ministry of Science and Higher Education of Russian Federation under agreement 075-15-2021-583. The vertical structure of O<sub>3</sub> and HNO<sub>3</sub> derivation and analysis was supported by the Russian Foundation for Basic Research, project number 20-05-00627.

## References

1. Solomon, S., Qin, D., Manning, M., Chen, Z., Marquis, M., Averyt, K.B., Tignor, M., Miller, H.L.: (eds.) Contribution of Working Group I to the Fourth Assessment Report of the Intergovernmental Panel on Climate Change. Cambridge University Press, Cambridge (2007).
2. Balis, D.S. An update on the dynamically induced episodes of extreme low ozone values over the northern middle latitudes. *Int. J. Remote Sens.* 32 (24), 9197–9205 (2011).
3. Timofeyev, Yu.M., Smyshlyayev, S.P., Virolainen, Ya.A., Garkusha, A.S., Polyakov, A.V., Motsakov, M.A., Kirner, O.: Case Study of Ozone Anomalies over Northern Russia in the 2015/2016 Winter: Measurements and Numerical Modeling. *Annales Geophysicae* 36 (6), 1495–1505 (2018).
4. Manney, G. L., Livesey, N.J., Santee, M.L., Froidevaux, L., Lambert, A., Lawrence, Z.D., Millán, L.F., Neu, J.L., Read, W.G., Schwartz, M.J., Fuller, R.A.: Record-Low Arctic Stratospheric Ozone in 2020: MLS Observations of Chemical Processes and Comparisons with Previous Extreme Winters. *Geophys. Res. Lett.* 47 (16), e2020GL089063 (2020).
5. Bernhard, G.H., Fioletov, V.E., Grooß, J.U., Ialongo, I., Johnsen, B., Lakkala, K., Svenby, T.: Record-Breaking Increases in Arctic Solar Ultraviolet Radiation Caused by Exceptionally Large Ozone Depletion in 2020. *Geophys. Res. Lett.* 47 (16), e2020GL090844 (2020).
6. De Mazière, M., Thompson, A.M., Kurylo, M.J., Wild, J.D., Bernhard, G., Blumenstock, T., Braathen, G.O., Hannigan, J.W., Lambert, J.-C., Leblanc, T., McGee, T.J., Nedoluha, G., Petropavlovskikh, I., Seckmeyer, G., Simon, P.C., Steinbrecht, W., Strahan, S.E.: The Network for the Detection of Atmospheric Composition Change (NDACC): history, status and perspectives. *Atmos. Chem. Phys.* 18 (7), 4935–4964 (2018).
7. NDACC database homepage, <https://www-air.larc.nasa.gov/missions/ndacc/data.html>, last accessed 2022/11/02.
8. Hase, F., Hannigan, J., Coffey, M., Goldman, A., Hopfner, M., Jones, N., Rinsland, C., Wood, S.: Intercomparison of retrieval codes used for the analysis of high-resolution, ground-based FTIR measurements. *J. Quant. Spectrosc. Radiat. Transfer* 87 (1), 25–52 (2004).
9. Virolainen, Y., Timofeyev, Y., Polyakov, A., Ionov, D., Poberovsky, A.: Intercomparison of satellite and ground-based measurements of ozone, NO<sub>2</sub>, HF, and HCl near Saint Petersburg, Russia. *Int. J. Remote Sens.* 35 (15), 5677–5697 (2014).
10. Virolainen, Ya.A., Timofeyev, Yu.M., Poberovskii, A.V., Kirner, O., Hoepfner, M.: Chlorine nitrate in the atmosphere over St. Petersburg. *Izv., Atmos. Ocean. Phys.* 51 (1), 49–56 (2015).
11. Virolainen, Ya.A., Timofeyev, Yu.M., Polyakov, A.V., Ionov, D.V., Kirner, O., Poberovskii, A.V., Imhasin, H.Kh.: Comparing data obtained from ground-based measurements of the total contents of O<sub>3</sub>, HNO<sub>3</sub>, HCl, and NO<sub>2</sub> and from their numerical simulation. *Izv., Atmos. Ocean. Phys.* 52 (1), 57–65 (2016).
12. Polyakov, A.V., Timofeyev, Yu.M., Poberovskii, A.V., Yagovkina, I.S.: Seasonal Variations in the Total Content of Hydrogen Fluoride in the Atmosphere. *Izv., Atmos. Ocean. Phys.* 47 (6), 760–765 (2011).
13. Virolainen, Y.A., Timofeyev, Y.M., Poberovsky, A.V.: Intercomparison of satellite and ground-based ozone total column measurements. *Izv. Atmos. Ocean. Phys.* 49 (9), 993–1001 (2013).
14. Smyshlyayev, S.P., Virolainen, Y.A., Motsakov, M.A., Timofeev, Yu.M., Poberovskiy, A.V., Polyakov, A.V.: Interannual and seasonal variations in ozone in different atmospheric layers over St. Petersburg based on observational data and numerical modeling. *Izv. Atmos. Ocean. Phys.* 53 (3), 301–315 (2017).
15. Nerobelov, G, Timofeyev, Y, Virolainen, Y, Polyakov, A, Solomatnikova, A, Poberovskii, A, Kirner, O, Al-Subari, O, Smyshlyayev, S, Rozanov, E.: Measurements and Modelling of Total Ozone Columns near St. Petersburg, Russia. *Remote Sensing*. 14 (16), 3944 (2022).
16. Rodgers, C.D.: Inverse methods for atmospheric sounding: Theory and practice. World Scientific Publishing Co. Pte. Ltd., Singapore (2000).
17. Virolainen, Y.A., Polyakov, A.V., Kirner O.: Optimization of procedure for determining chlorine nitrate in the atmosphere from ground-based spectroscopic measurements. *J. Appl. Spectr.* 87 (2), 319–325 (2020).

18. Timofeyev, Y., Virolainen, Y., Makarova, M., Poberovsky, A., Polyakov, A., Ionov, D., Osipov, S., Imhasin, H.: Ground-based spectroscopic measurements of atmospheric gas composition near Saint Petersburg (Russia). *J. Mol. Spectrosc.* 323, 2–14 (2016).
19. Polyakov, A., Poberovsky, A., Makarova, M., Virolainen, Y., Timofeyev, Y., Nikulina, A.: Measurements of CFC-11, CFC-12, and HCFC-22 total columns in the atmosphere at the St. Petersburg site in 2009–2019. *Atmos. Meas. Tech.* 14 (8), 5349–5368 (2021).
20. Boone, C.D., Bernath, P.F., Cok, D., Jones, S.C., Steffen, J.: Version 4 retrievals for the atmospheric chemistry experiment Fourier transform spectrometer (ACE-FTS) and imagers. *J. Quant. Spectrosc. Rad. Transf.* 247, 106939 (2020).
21. Molina, L.T., Molina, M.J.: Production of chlorine oxide ( $\text{Cl}_2\text{O}_2$ ) from the self-reaction of the chlorine oxide (ClO) radical. *J. Phys. Chem.* 91 (2), 433–436 (1987).
22. Solomon, S., Haskins, J., Ivy, D., Min, F.: Fundamental Differences Between Arctic and Antarctic Ozone Depletion. *Proceedings of the National Academy of Sciences of the USA* 111, 6220–6225 (2014)
23. Toumi R., Jones R.L., Pyle J.A.: Stratospheric ozone depletion by  $\text{ClONO}_2$  photolysis. *Nature* 365 (6441), 37–39 (1993).
24. Chipperfield, M.P., Burton, M., Bell, W., Paton Walsh, C., Blumenstock, T., Coffey, M.T., Hannigan, J.W., Mankin, W.G., Galle, B., Mellqvist, J., Mahieu, M., Zander, R., Notholt, J., Sen, B., Toon, G.C.: On the use of HF as a reference for the comparison of stratospheric observations and models. *J. Geophys. Res.* 102 (D11), 12901–12919 (1997).
25. Hersbach, H., Bell, B., Berrisford, P., Hirahara, S., Horányi, A., Muñoz-Sabater, J., Nicolas, J., Peubey, C., Radu, R., Schepers, D., Simmons, A., Soci, C., Abdalla, S., Abellan, X., Balsamo, G., Bechtold, P., Biavati, G., Bidlot, J., Bonavita, M., De Chiara, G., Dahlgren, P., Dee, D., Diamantakis, M., Dragani, R., Flemming, J., Forbes, R., Fuentes, M., Geer, A., Haimberger, L., Healy, S., Hogan, R.J., Hólm, E., Janisková, M., Keeley, S., Laloyaux, P., Lopez, P., Lupu, C., Radnoti, G., de Rosnay, P., Rozum, I., Vamborg, F., Villaume, S., Thépaut, J.-N.: The ERA5 Global Reanalysis. *Quart. J. Royal Meteor. Soc.* 146 (730), 1999–2049 (2020).
26. Kopp, G., Berg, H., Blumenstock, T., Fischer, H., Hase, F., Hochschild, G., Hoepfner, M., Kouker, W., Reddmann, T., Ruhnke, R., Raffalski, U., Kondo, Y.: Evolution of ozone and ozone-related species over Kiruna during the SOLVE/THESEO 2000 campaign retrieved from ground-based millimeter-wave and infrared observations. *J. Geophys. Res.* 108 (D5), 8308 (2002).
27. Blumenstock, T., Kopp, G., Hase, F., Hochschild, G., Mikuteit, S., Raffalski, U., Ruhnke, R.: Observation of unusual chlorine activation by ground-based infrared and microwave spectroscopy in the late Arctic winter 2000/01. *Atmos. Chem. Phys.* 6 (4), 897–905 (2006).
28. Virolainen, Y.A., Polyakov, A.V. & Timofeyev, Y.M.: Analysis of the Variability of Stratospheric Gases Near St. Petersburg Using Ground-Based Spectroscopic Measurements. *Izv. Atmos. Ocean. Phys.* 57 (2), 148–158 (2021).
29. Khosrawi, F., Kirner, O., Sinnhuber, B.-M., Johansson, S., Höpfner, M., Santee, M. L., Froidevaux, L., Ungermann, J., Ruhnke, R., Woiwode, W., Oelhaf, H., Braesicke, P.: Denitrification, dehydration and ozone loss during the 2015/2016 Arctic winter. *Atmos. Chem. Phys.* 17 (21), 12893–12910 (2017).